Iranian Journal of Chemical Engineering

Journal Homepage: www.ijche.com

pISSN: 1735-5397
eISSN: 2008-2355

Regular Article

Fabrication and Characterization of Polysulfone-Graphene Oxide Mixed Matrix Membranes for the Natural Gas Treatment

R. Bakhshi [1], ***M. Keshavarz Moravaji*** [2*], ***A. Parvareh*** [3]

[1] *Department of Chemical Engineering, Borujerd Branch, Islamic Azad University, Borujerd, Iran*
[2] *Department of Chemical Engineering, Amirkabir University of Technology (Tehran Polytechnic), Tehran, Iran*
[3] *Department of Chemical and Petroleum Engineering, Razi University, Kermanshah, Iran*

ARTICLE INFO

Article history:
Received: 2022-06-04
Accepted: 2022-09-14
Available online: 2022-09-18

Keywords:
Membrane,
Gas Separation,
Mixed Matrix Membrane,
Graphene Oxide

ABSTRACT

The polysulfone mixed matrix membranes (MMM) with different concentrations of graphene oxide (0, 0.25, 0.5 wt % of the polymer) are fabricated by a phase separation method. The cross-sectional structures and their upper surface were assessed by the (SEM) surface roughness of the membranes assessed by (AFM). The mechanical and thermal stability of the fabricated membranes were evaluated as well. The separation of Carbon dioxide, nitrogen and methane from natural gas was considered. Also, by increasing the concentration of graphene oxide in the polymer matrix, the thickness of the spongy structure increases and the holes of the finger-like membranes are also destroyed. From the cross-sectional images of the outer surface of the MMM, it was concluded that an active selector layer was created on the lower surface of the membrane. The membrane tensile strength and the length of the membrane at fracture point increased slightly with an increase in the concentration of graphene oxide. Transition Glass temperature of the membrane increased by the addition of graphene oxide to the structure. From TGA analysis, in the presence of graphene oxide, the thermal stability improved. From the gas permeation test, by the addition of 0.25 % of graphene oxide to the polymer, CO_2 permeability was increased from 61.22 GPU to 76.04 GPU, while the addition of 0.5 wt % resulted in a lower permeability (69.55 GPU). The Nitrogen gas permeation flux of membranes decreased from 10.93 GPU to 3.91 GPU by the addition of 0.50 wt % of graphene oxide. The Methane gas permeation flux is reduced from 11.31 GPU to 6.95 GPU and 4.92 GPU by the addition of 0.25 % and 0.50 % of graphene oxide respectively. In conclusion, an increase in the concentration of graphene oxide increased the carbon dioxide selectivity.

DOI: 10.22034/ijche.2022.344393.1442 URL: http://www.ijche.com/article_157491.html

1. Introduction

Applying polymeric membranes for the gas

*Corresponding author: moraveji@aut.ac.ir (M. Keshavarz Moraveji)

separation is a major concern among researchers. Limitations and drawbacks like the low thermal and chemical resistance and the swelling of polymeric membranes have made researchers modify the structure of membranes applied in the gas separation processes.

Inorganic membranes are able to withstand high temperature and are durable compared to the polymer membranes. Researchers seek to find methods to achieve the benefits of both polymeric and inorganic membranes in a simultaneous manner. Mixed membrane matrixes (MMM) that have been fabricated prevail over the restriction and drawbacks of both membranes. To fabricate MMMs, inorganic fillers are applied in the polymer membrane matrix. In recent years, MMMs have been used for different applications like the gas separation, water desalinization, heavy metals removal from water, gas absorption and discharges.

Graphene, known as a low permeability filler, has not been weighed in the construction of MMMs for the separation of gas. Natural graphene is an inert substance and due to its ability to propagate in the solvents and reaction being very low, it does not form a homogeneous mixture with the polymer. In order to increase the stability of graphene in solvents and form a bond with the polymer chain, introducing application groups on the graphene surface is essential. it is a graphene-based nanoparticle, and is linked to oxygen-bound groups. Active cell groups, like carboxyl and hydroxyl in graphene oxide, can propagate in the polymer matrix in a proper manner which can improve the membrane gas separation properties [1, 2]. Applying graphene oxide for the MMM fabrication, creates a pathway for small gas molecules to pass but prevents the large gas molecules passing [3, 4]. Recent studies have shown, the nanoparticles of graphene oxide in the structure of the membranes increased the mechanical and thermal durability of the membranes [5-9]. Researchers have addedgraphene oxide to the structure of the polysulfide hollow fiber membrane, and therefore, the tensile strength and length stretching increased during the membrane breakage by 36.3 % and 8.79 % respectively [10]. It is also observed that the graphene polyculture-oxide mixed matrix membrane has a high thermal stability and its mechanical properties have increased when 0.25 % of graphene oxide was added to the matrix [11].

According to the latest studies, graphene oxide is rarely applied in improving the structure of polymeric membranes for the nitrogen/carbon dioxide/methane separation. In this study, polysulfone MMMs were prepared by applying graphene oxide as a filler additive. After assessing the structure and specifications of the membranes, they were applied in the nitrogen/carbon dioxide/methane gas separation.

2. Experiments

2.1. Primitive materials

The membrane (PSd Udel P-3550, Chemicals Amco, USA) is applied as the base polymer for the membrane fabrication. The reason for selecting this polymer is its good mechanical stability and easy processing [12-15]. The N-methyl-acetamide solvents of (DMAC > 95 %) and tetrahydrofuran of (THF ≥ 99.5 %) were procured from Merck, and used as the solvents. Natural graphene sheets (≤ 22 μm), ethanol and ($KMnO_4$) were purchased from Aldrich. (H_2SO_4, 94-98 wt %), (HCl) and (H_2O_2, 32 wt %) were catered from Merck, Germany. Distilled water was made in the laboratory and utilized as the coagulant in the process of

fabricating membranes.

2.2. Synthesis of graphene oxide

The oxidation of graphite was applied to prepare graphene oxide by the modified Hummer method [3, 16]. Here, 3 gr of powder graphite was dissolved in 100 ml of H_2SO_4; the solution mingled in an ice bath at 0 °C; 10 gr of potassium permanganate was added to the solution in a slow manner and the solution was stirred at below 10 °C for 3 hours. The temperature was increased to 40 °C and the solution was stirred for 35 minutes in a vigorous manner. 150 ml of distilled water was added to the solution and it was heated to about 100 °C where it was riled for 20 minutes at this temperature. Then 500 ml of distilled water and 15 ml of hydrogen peroxide were added to the solution. The solution was placed on an ultrasonic apparatus for 1 hour in order to separate the large graphene oxide grains. The mixture was filtered and then rinsed by distilled water containing 3 vol % of sulfuric acid to remove metal ions. The produced graphene oxide was dried in an oven for 8 hours and then was grinded to obtain a graphene oxide powder.

2.3. Preparing the polymer solutions

In order to fabricate MMMs, three types of the polymer solutions were prepared as follows:

The first solution was free of graphen oxide, where the solution contained polysulfone polymer (30 wt %), dimethyl acetamide (35 wt %), tetrahydrofuran (30 wt %) and ethanol (5 wt %). The ratios related to the polymer solutions are given elsewhere [12, 17-18]. To prepare 100 g of this solution, first, 35 g of the DMAC solution was poured into a glass bottle and 30 g of tetrahydrofuran was added. When the mixture of solvents in the bottle was being stirred by a mechanical riler, 30 g of polymer was gradually added to the solvent. The gradual addition of the polymer prevents the agglomeration of the polymer seeds. The solution was riled for 24 hours to dissolve all the polymer in the solvent. After making sure that all polymer seeds in the solvent were dissolved, 5 g of ethanol was added to it and riled again for 2 hours to achieve a homogeneous solution. To remove the air bubbls in it, the solution was placed on an ultrasonic apparatus for 60 minute and then kept at ambient temperature for 1 day.

The second solution was prepared using graphene oxide by 0.25 % (w/w) of the polymer. To prepare 100 g of this solution, 35 g of dimethyl acetamide was first poured into a glass bottle, then graphene oxide was added to the dimethyl acetamide solution. The bottle containing the solution was placed on an ultrasonic apparatus for 1 hour so that the particles will be dispersed in the solvent. For the better dispersion of graphene oxide particles in the solution of DMAc, the suspension solution was placed on a sonicator micro-tip (505 watts, 3 s) for 5 minutes. Then 30 g of the tetrahydrofuran solvent was added to the solution and it was stirred mechanically for 60 minute. 30 g of polysulfone was gradually added to this solution and the resulted solution was stirred for 24 hours to dissolve all the polymer in this solution. Finally, 5 g of ethanol was added to it and the bottle of the solution was placed on an ultrasonic apparatus for 1 hour to discharge the air bubbles. To make sure that all air bubbles in the polymer solution were discharged, the solution was placed at ambient temperature for 24 hours before use.

The preparation of the third solution was similar to the second one, but the polymer solution was prepared using graphene oxide at a rate of 0.5 % (w/w) of the polymer. The

proportional compositions of the prepared solutions are shown in Table 1.

Before applying the prepared polymer solutions to fabricate the membrane, the viscosity of solutions was measured by a viscometer.

Table 1
Proportional composition of materials in the polymer solution.

Solution name	Polymer (wt %)	DMAC (wt %)	THF (wt %)	Ethanol (wt %)	GO (wt % of polymer)
S1	30	35	30	5	-----
S2	30	35	30	5	0.25
S3	30	35	30	5	0.50

2.4. Membrane construction via a phase separation method

To make the membranes, the polymer solution was spread on a glass sheet and was strewn as a film with a balanced thickness. The solution was kept on the sheet for 120 seconds to reach to a membrane with a dense skin. Then the plate was plunged in a container full of distilled water at ambient temperature to accomplish the phase separation process. The fabricated membrane was spilled from the glass sheet and kept in distilled water for 1 day. Then the flat membrane sheet was dried at ambient temperature.

2.5. Specification of the synthesized graphene oxide

2.5.1. Transmission Electron Microscopy (TEM)

The structure of the synthesized graphene oxide surface was distinguished through (TEM, Zeiss EM900, Germany). For this purpose, a small amount of graphene oxide was poured into ethanol and the solution was placed on an ultrasonic device for 60 minute to disperse graphene oxide into the ethanol. The resulting suspension was kept at the environment temperature for 15 minutes. Then some of the resulted solution was placed into the microscope to capture an image of the graphene oxide structure.

2.5.2. Fourier Transform Infrared Spectroscopy (FTIR)

The chemical structure of graphene oxide was analyzed by FTIR spectroscopy. For this purpose, the samples were placed in a dryer at 60 °C overnight to allow the excess water to be discharged. The samples were then grinded along with potassium bromide at the ratio of 1:10.

2.6. Characterization of the fabricated MMM

2.6.1. Scanning Electron Microscope (SEM)

To display cross-sectional and surface images of the fabricated membranes, sthe canning electron microscopy (TM3000, HITACHI, Japan) was used. Small pieces of 5 × 5 cm membranes were cut in liquid nitrogen, so that the cross-sectional structure would break with no failure. The broken parts were placed in an oven at 60 °C and for 2 hours for the removal of moisture from the membranes pores. The membrane samples were then coated with platinum to enhance the reflectivity of electrons shifted by the scanning electron microscope and to provide better quality images.

2.6.2. Atomic Force Microscopy (AFM)

To assess the membrane surface roughness and determine the average roughness (Ra), the atomic force microscopy (AFM, SPA-300 HV, Seiko, Japan) was applied. For this purpose, small pieces of 5 × 5 cm membranes were cut and the surface roughness was assessed by AFM.

2.6.3. Mechanical stability of the membranes

The extra length and rigidity tensile at breaking point of the MMM were measured by ASTM D3930 through a tensile test machine (LRX 2 Llyod SKN). For this purpose, membranes were cut to pieces of 6 cm in length and placed in the device.

2.6.4. Differential Scanning Calorimetry (DSC)

The transition temperature (Tg) of the produced MMM was delineated by a scanning differential calorimeter model (DSC, Mettler Toledo DSC, 822e). The samples were heated from about 30 °C to 410 °C at an intensity of 11 °C/min, after which the cooling took place in the reverse manner. The heating and cooling operation was run twice: the first was to calibrate the sample and the second was to determine Tg.

2.6.5. Thermal Gravimetric Analysis (TGA)

The thermal stability analysis of graphene oxide and the prepared membranes were conducted through a thermal gravimetric analyzer (TGA, Perkin Elmer). The sample was heated until a change in its weight was observed. The sample was heated within 32 °C to 805 °C at intensity of 12 °C/min at 25 ml/min of the flow rate of nitrogen.

2.7. Membrane gas separation test

The separation performance of the membranes for carbon dioxide, nitrogen and methane gases was conducted through a gas permeability apparatus. A circular piece of the membrane impressive surface zone of 13 cm² was placed in a stainless steel module. The gas was injected to the module at 24 °C and 5 bar pressure. Using a soap bubble flow meter, the permeability of the gas flow into the membranes was measured. The gas permeation flux (P/L) was calculated through Eq. (1) [19]:

$$P / L = Q / (A.\Delta P) \quad (1)$$

P is the flux of the gas permeability (cm^3/s), A is the effective surface of the membrane (cm^2), ΔP is the pressure difference between the two sides of the membrane (cmHg), L is the thickness of the membrane (cm) and Q is the permeated gas flow (cm^3/s).

The ideal selectivity, α_{ij}, is given as [20]:

$$\alpha_{ij} = P_i / P_j \quad (2)$$

The apparatus is showing in Figure 1.

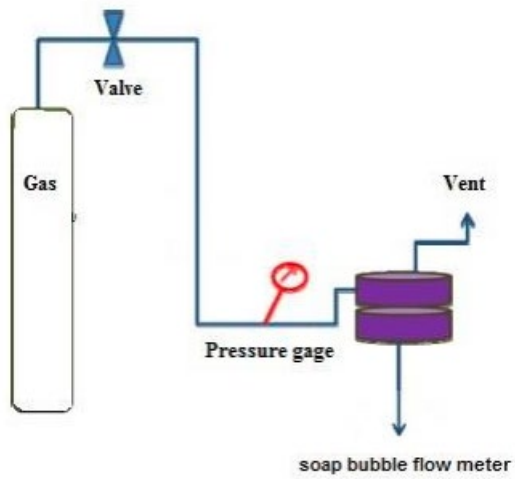

Figure 1. Testing apparatus.

3. Results and discussion

3.1. Structure and specifications of the synthesized graphene oxide

The TEM images of the synthesized graphene oxide with various magnifications are

displayed in Figure 2. The TEM image indicates that graphene oxide was synthesized through a smooth and transparent manufacturing process.

The FTIR of graphene oxide and spectrum of graphite are shown in Figure 3. There is no significant peak in the graphite spectrum, while the presence of various types of oxygenating agents in graphene oxide was confirmed by the IR spectrum.

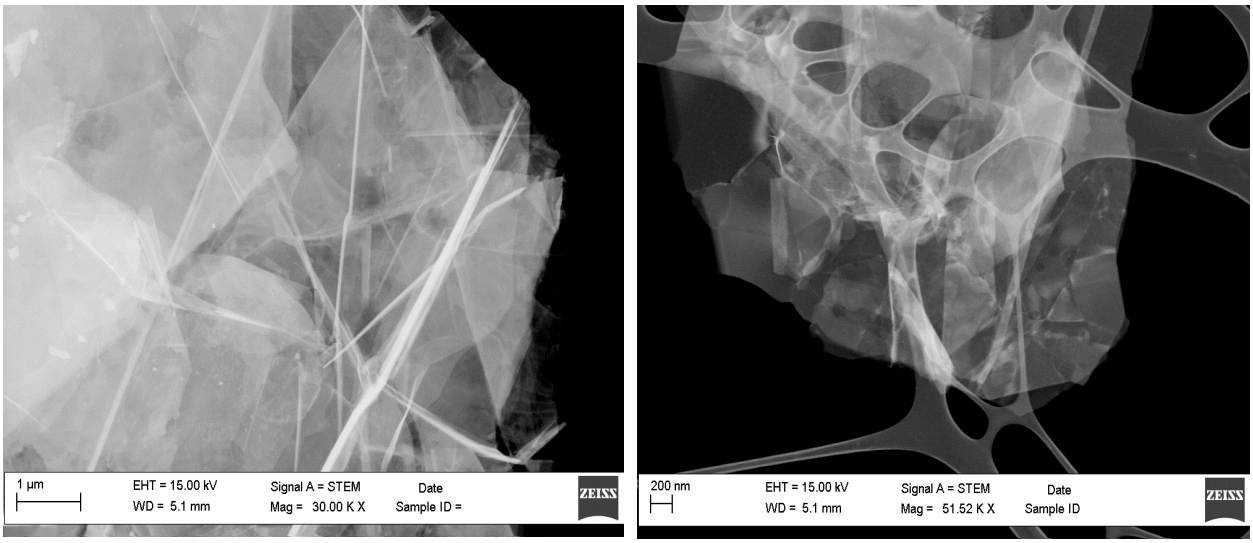

Figure 2. TEM picture of the synthesized graphene oxide.

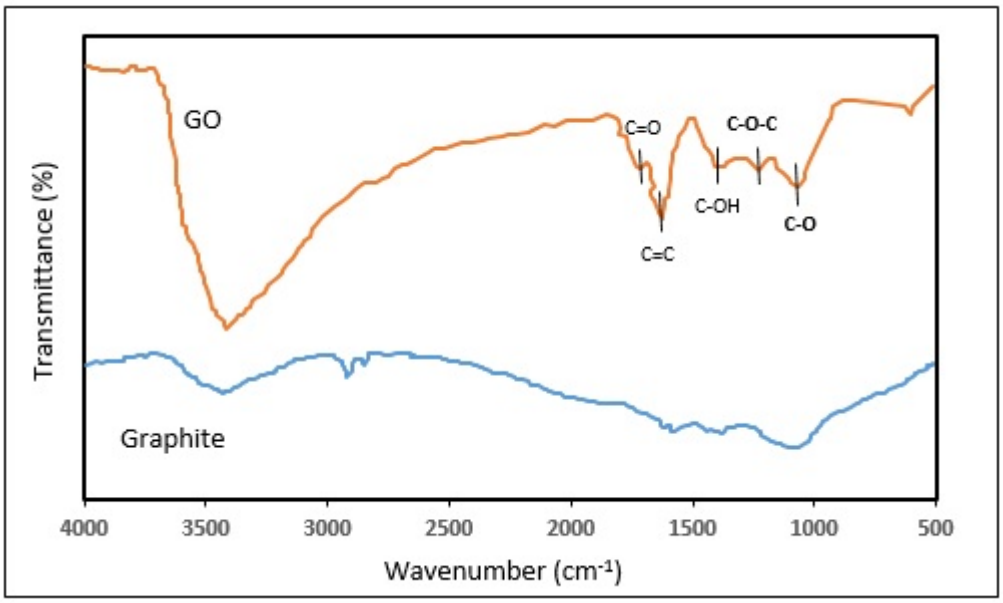

Figure 3. FTIR spectra of graphite and graphene oxide.

For graphene oxide at the spectra between 3000 (cm^{-1}) and 3700 (cm^{-1}), an absorption band is expanded, which is related to the stretching vibrations of the O-H group on the surface or the water molecules absorbed in the layer's graphene oxide. This absorption band includes several stretching O-H functional groups indicating the functional groups of O-H being present in the form of alcohol, phenol, or carboxylic acid at the surface of

graphene oxide [21, 22]. Two couriers, appeared at 1725 cm^{-1} and 1605 cm^{-1}, could be the tensile vibrations related to the double bond of hydrocarbons.

The TGA results of the graphene oxide and natural graphite are shown in Figure 4.

The thermal degradation of graphene oxide is related to the functional groups connected to the surface. The first weight loss at 120 % occurred at the temperature of 120 °C which was related to the removal of water in graphene oxide [23]. The second weight loss occurred within 120 °C and 250 °C, at a rate of 27 %, which was due to the removal of oxygen in the agent group [24]. The third weight loss occurred within 245 °C and 855 °C, due to the removal of the residues of the stable oxygen in the functional groupsexisting in the structure of the main graphene oxide, and the pyrolysis of the unstable carbon-oxide in the graphene structure [8, 25]. The general weight loss of 59 % occurred at 900 °C. The TGA analysis revealed that graphene oxide had more thermal instability than natural graphite, indicating that graphene oxide was successfully synthesized.

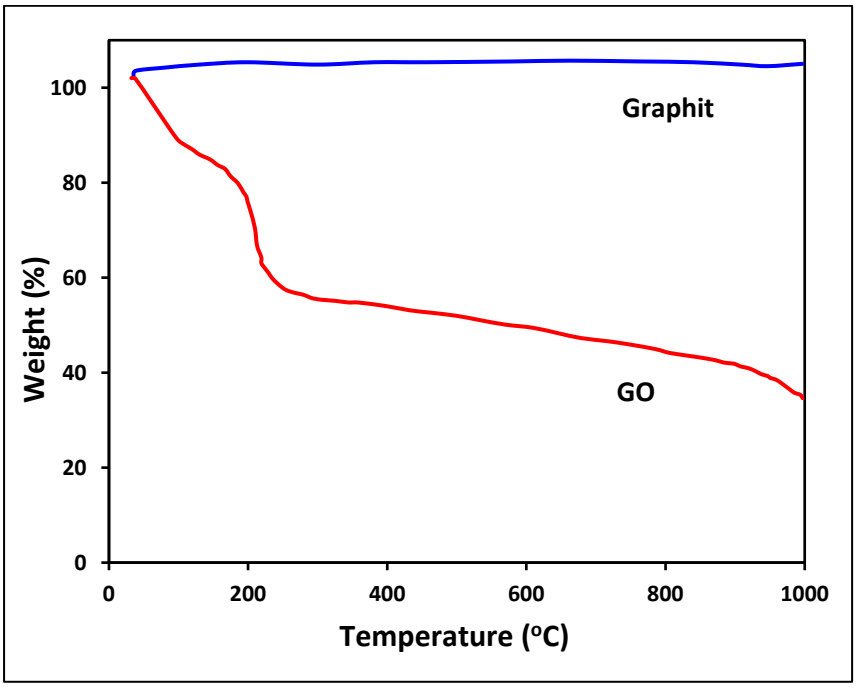

Figure 4. Thermal gravity analysis of graphene oxide and graphite.

3.2. Structure and specification of the membranes

In this study, three polysulfone solutions with various concentrations of 0, 0.25, 0.5 % w/w of graphene oxide, named M1, M2 and M3 respectively, were prepared. The membranes were manufacture by the phase separation process. The viscosities of the prepared solutions were measured and given in Table 3. As it can be seen, the viscosity of the solution increased.

Table 3
Viscosity of the polymer solutions.

Solution name	Viscosity (cP)
S1	8919
S2	11688
S3	13549

3.2.1. Morphology of the surface of the prepared membranes

The morphology of the surface of the fabricated membranes was analyzed through

an atomic microscopy force (Figure 5). The coarseness of the Surface (Ra) membranes are shown in Table 4.

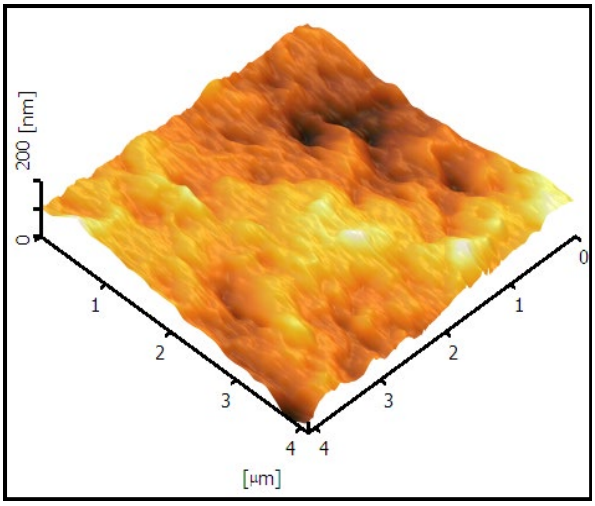

(A)

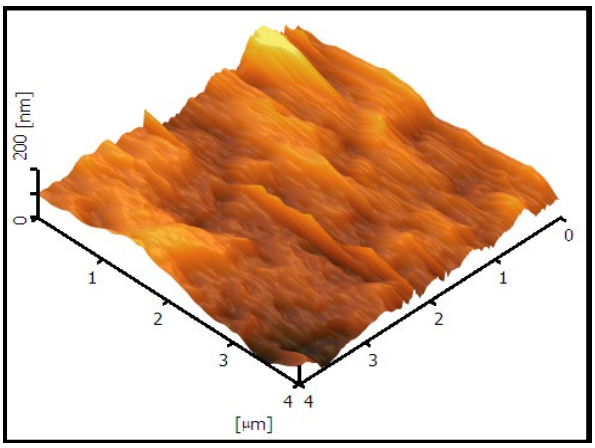

(B)

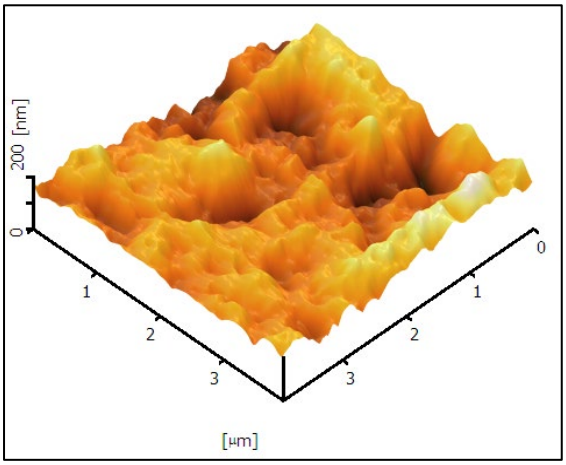

(C)

Figure 5. AFM images of the membrane surface, (A) pure polysulfone, (B) 0.24 wt % of GO and (C) 0.52 wt % of GO.

Table 4

Average surface roughness of the membranes.

Membrane name	GO (wt %)	Mean roughness (R_a) (nm)
M1	0	12.59
M2	0.25	14.02
M3	0.50	17.33

According to the obtained results, by increasing the concentration of graphene oxide in the polymeric solution the roughness of the surface of membranes increases. Moreover, the increment of the roughness of the membrane surface can be attributed to the growth of the exchange rate of solvent/non-solvent during the phase separation process [4, 6]. Changing the solvent may result in the formation of polymer spheres or nodes, which results in a mild surface roughness of the membrane. This can lead to the development of the membrane porosity.

3.2.2. Structural morphology of the prepared membranes

The SEM is used to appraise cross-sectional frame membranes images as shown in Figure 6.

The images of the transverse section show that, the apt membranes contain a dense active layer of a thin sponge-like substrate and a thick fuzzy layer with large cavities. Using 2 min air gap time before the immersion of the membrane in the gelation bath, causes the evaporation of THF resulting in the formation of a selective thin layer on the membrane surface [17]. Moreover, the foundation of the spongy and finger-like structure during the wet phase separation process is pertinent to exchange the solvents (DMAc, THF, Etoh), for the water existing in the coagulation bath. In general, when the rate of the phase separation process is high, the possibility of the structure

being in the form of the insoluble fingure-like is high, like when a dactyl structure is formed, whereas the formation of the sponge-like structure is related to a low rate of the phase separation [26].

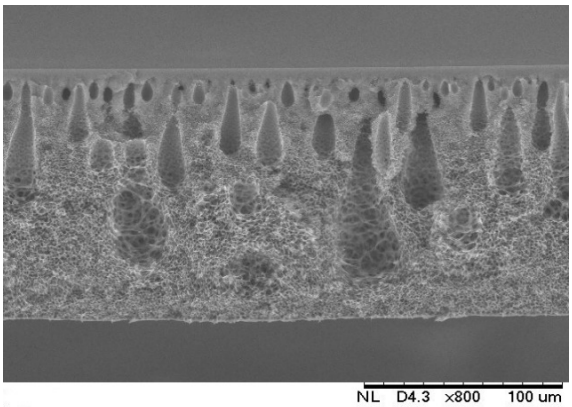

(A)

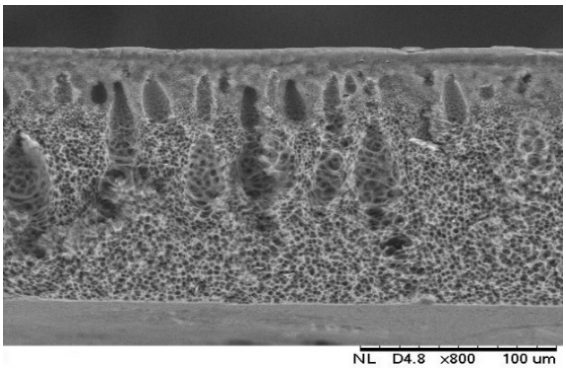

(B)

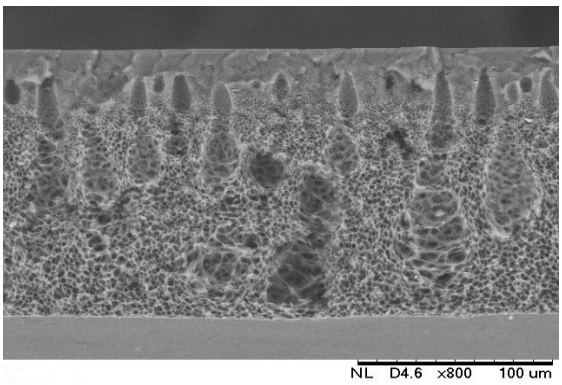

(C)

Figure 6. Cross-sectional images of the prepared membranes, (A) Pure polysulfone, (B) 0.3 wt % of GO, (C) 0.55 wt % of GO.

The formation of a finger-like or sponge-like structure in the phase separation process depends on the viscosity and thermodynamic instability of the polymer solution, where increasing the viscosity of the polymer solution causes a decrease in the rate of the phase separation process, and results in a sponge-like structure. From Figure 6, it can be seen that an increase in graphene oxide compactness in the polymer leads to the improvement of the thickness of the sponge-like structure and disappearance of the dactyl-like cavities. From Table 3, it can be seen that an increase in the density of graphene oxide in the polymer increased the viscosity of the solution, thus the delay in the phase separation process improved the sponge-like thickness. Images of membranes were taken at the magnification of 5K, as illustrated in Figure 7, and the width of the selector layers was measured. The thickness of the selector layers of the pure polysulfone membrane was about 132 nm which has been higher than the membranes prepared by graphene oxide. By adding 0.25 % of graphene oxide to the polymer solution, the membrane layer thickness decreased to 86 nm. While by increasing the concentration of graphene oxide to 50 % the selector layer thickness increased to 102 nm. It is well-known that a thin selective layer is highly contributive to the membrane gas separation properties.

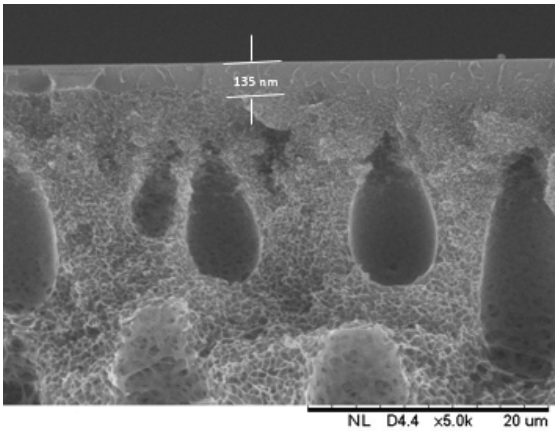

(A)

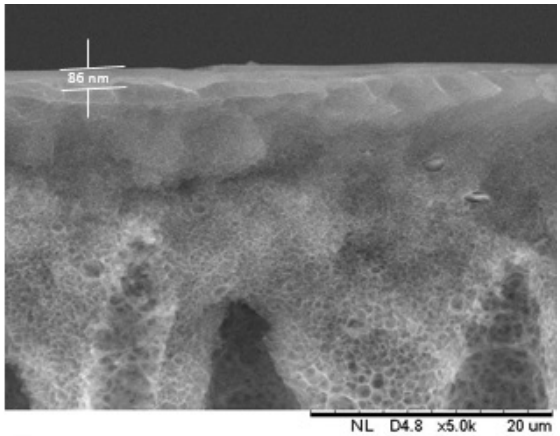

(B)

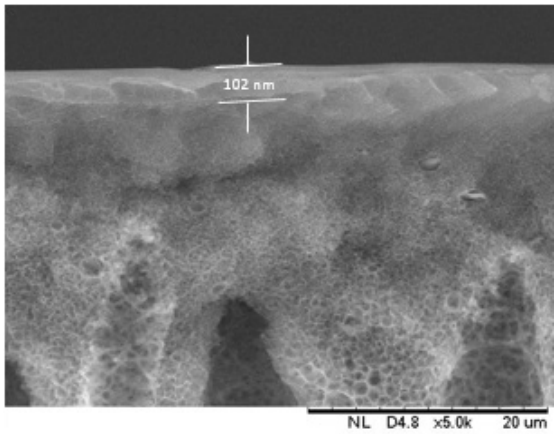

(C)

Figure 7. Intermittent images membranes at 5K homage, (A) Pure polysulfone, (B) 0.3 wt % GO, (C) 0.50 wt % GO.

Outer surface pictures of the prepared membranes with different thicknesses are displays in Figure 8. The pure PSF membrane showed a more porous structure compared to MMM. Using graphene oxide in the polymer solution formed an integrated thin selector layer at the early stages of the dry phase separation process. In addition, to form a porous sublayer, this integrated layer was involved in the formation of a sublayer with the optimum thickness during a wet phase separation process.

3.2.3. Mechanical stability of the prepared membranes

The mechanical stability of membranes, tensile strength and elongation at the fracture point are measured and the results are given in Table 5.

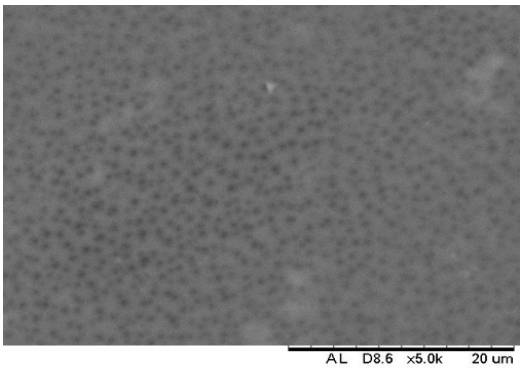

(A)

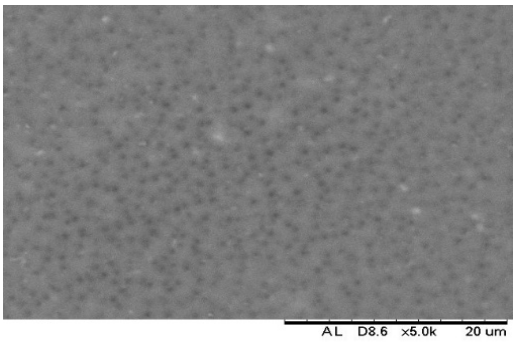

(B)

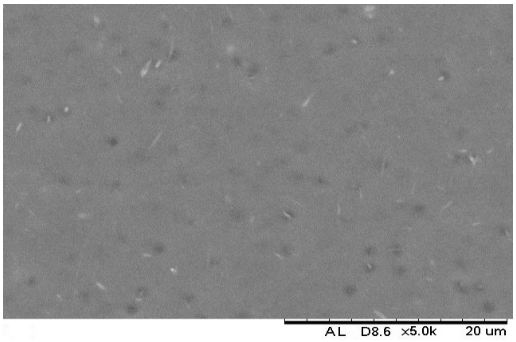

(C)

Figure 8. SEM picture of the outer surface of membranes, (A) Pure polysulfone, (B) 0.25 wt % of GO, (C) 0.50 wt % of GO.

Table 5
Fortification tensile and elongation.

Membrane name	Ts (MPa)	E break (cm)
M1	1.23	6.51
M2	1.80	6.89
M3	2.25	7.12

As it can be seen, by increasing the concentration of graphene oxide, the formation tensile and elongation of the membrane slightly increase. It deduced the mechanical durability of the membranes. In fact, this slight increase in the mechanical stability reflects the good dispersion of graphene oxide at the membrane structure. The obtained results are consistent with the ones reported previously [11, 7].

Unlike the results obtained in the present study, some studies have shown that the elongation at the break point of the mixed matrix membrane is reduced by increasing the tensile strength of the membrane [28, 29]. This decrease is due to the destruction of the fetter polymer order caused by the presence of fillers in the polymer matrix, mainly by the rigidity of the polymer around the filler. Contrary to the results of previous studies, it is observed that enhancing the concentration of graphene oxide in the membrane structure causes the membrane length at the breaking point to increase. The reason for this phenomenon can be considered the addition of graphene oxide. Moreover, the proper distribution of graphene oxide and its good interaction with the polymer matrix, increase the mechanical strength. As it was found before, the active agent groups attached to graphene oxide contribute to the interphase interactions and strong bonds between graphene oxide and polymer matrix [20].

3.2.4. TGA and DSC Analysis of membranes

(Tg) of the fabricated membranes was determined through the differential scanning calorimetry. The interactions between graphene oxide and polysulfone can be predicted by applying the Tg values. The results of Tg and the glass transitiontemperature of the fabricated membranes are shown in Table 6.

Table 6
Tg and temperature parsing.

Membrane name	Tg (°C)	Td (°C)
M1	188.23	498
M2	213.08	513
M3	216.59	538

As it is observed in Table 6, by the addition of graphene oxide to the membrane structure, Tg increased considerably due to the strong bond between polysulfone and graphene oxide. These strong bonds are due to the active agent groups which have established a good bond with the polymer [23]. These bonds have prevented the mobility of polymer chains and therefore increased the Tg value. In another study, a reduction in Tg was observed by adding halothon nanotubes (HNT) to the polymer matrix [30].

The TGA graphs of pure membranes and MMMs are shown in Figure 9. The results indicate that the membrane decomposition temperature has increased. As it is observed, the pure membrane reveals weaker weight loss than the MMM. The weight loss for M1, M2 and M3 membranes occurs at 498, 513, and 538 °C respectively. Therefore, the addition of graphene oxide to the membrane matrix improves the thermal stability. For all membranes, slight weight loss was observed at temperatures below 495 °C. The reason for such a reduction was the destruction of the polymer matrix [11].

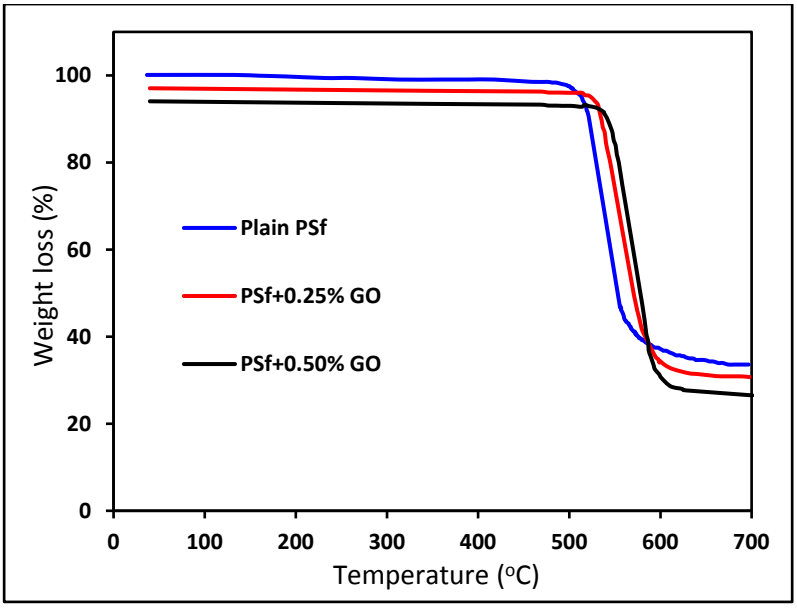

Figure 9. TGA graphs of the prepared membranes.

3.3. Investigating the performance of MMMs in the gas separation

The gas permeation in the membranes for carbon dioxide, nitrogen, and methane at the constant pressure of 5 bar and 24 °C are measured and results are display in Figure 10. The flux of carbon dioxide increased, while the nitrogen and methane gas permeation decreased. The obtained results indicated that the MMMs with 0.25 % (M2) and 0.5 % (M3) of graphene oxide have 24.2 % and 13.6 % higher carbon dioxide permeation flux respectively, the Nitrogen permeation flux in M2 and M3 membranes decreased 76 % and 179.5 % respectively. In addition, the methane permeation flux in M2 and M3 membranes decreased by 62.7 % and 129.9 % respectively.

As it is observed, the flux reduction of nitrogen was higher than that of methane gas. The ideal solubility of nitrogen gas is reported to be much lower than that of carbon dioxide [31]. Observed SEM images that the skin layer of the pure membrane was thicker and has more pores compared to the MMMs.

It is proved that π-π grains existing in graphene oxide tend to be highly polarized [10]. The permeation flux of the carbon dioxide gas increased by adding 0.25 % of graphene oxide to the polymer matrix. As shown in Figure 7, the thickness of the layer of the pure polysulfone membrane was 132 nm. By adding 0.25 % and 0.5 % of graphene oxide to the polymer solution, the thickness of the selector layer relatively decreased. Thickening of the density of the selector layer prevents the carbon dioxide passing and decreases the permeability.

As it is observed in Figure 10, the permeability flux of carbon dioxide was 61.22 GPU for the pure membrane, which reached to 76.04 GPU by adding 0.25 % of graphene oxide to the polymer matrix. The addition of 0.5 % of graphene oxide resulted in the flux reduction to 69.55 GPU. An increase in the concentration of graphene oxide up to 0.5 % resulted in the reduction of the carbon dioxide permeation flux, which exceeded the amount of the carbon dioxide flux permeation in the polymer without graphene oxide.

The N_2 flux permeation is lower than that of carbon dioxide, where it was 10.93 GPU for the pure membrane and 3.91 GPU for the

membrane fabricated with 0.5 % of graphene oxide. The methane gas permeation flux was 11.31 GPU for the pure membrane and reached 6.95 GPU and 4.92 GPU for the membranes fabricated with 0.25 % and 0.5 % of graphene oxide respectively. The carbon dioxide selectivity of the prepared membranes is shown in Figure 11.

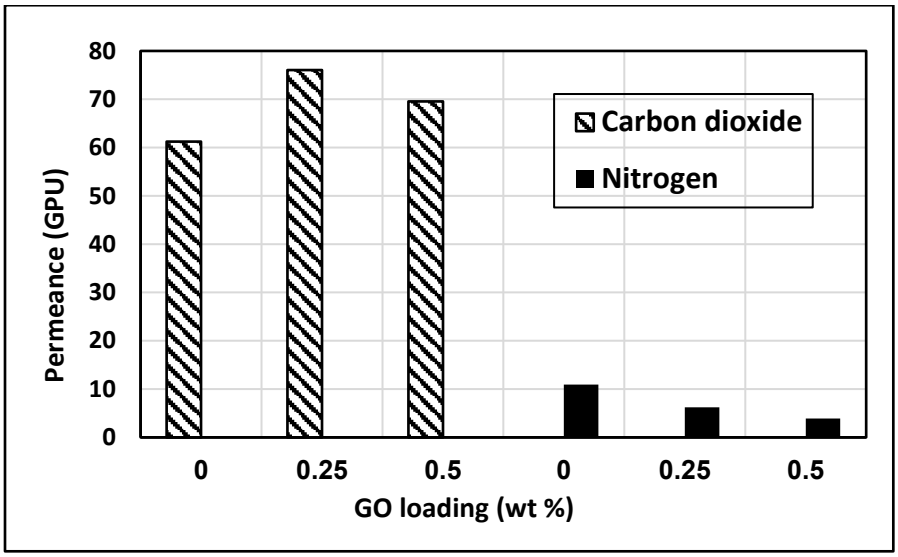

Figure 10. Permeability of carbon dioxide, nitrogen and methane.

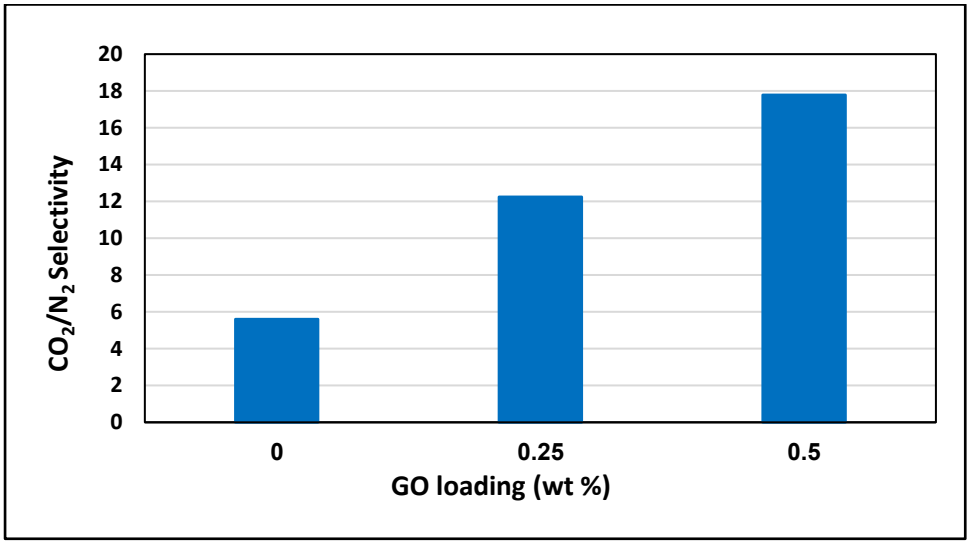

Figure 11. Carbon dioxide selectivity in relation to nitrogen and methane.

An increase in the concentration of graphene oxide increased the CO_2 selectivity of the membranes. In the explanation of the results of the membrane surface images it was explained that by adding graphene oxide to the polymer solution, a thin monolithic layer of the integrated monolith was formed. The inert gas molecules like nitrogen did not pass, which resulted in the improvement of the membrane selectivity. According to Figure 11, for M1, M2 and M3 membranes, the amounts of carbon dioxide selectivity for nitrogen are 5.60, 12.24 and 17.79 respectively. The amounts of carbon dioxide selectivity for methane were 5.41, 10.94 and 14.14 respectively.

According to the carbon dioxide and

nitrogen separation performance of the fabricated membranes, it can be deduced that adding graphene oxide to the polymer matrix improves the carbon dioxide permeation flux. Applying graphene oxide with the concentration of 0.25 % by weight in the polymer matrix can optimize the membrane structure, which cosequently increased the carbon dioxide permeation flux with a good selectivity compared to that of methane.

The gas permeation results obtained in the present study are compared with a number of published results and display in Table 7.

As it is observed, the fabricated membrane with 0.25 % of graphene oxide exhibited a better performance for the separation of carbon dioxide and nitrogen.

Table 7
Gas flux permeation.

Membrane type	Polymer	Filler	CO_2 permeance (GPU)	N_2 permeance (GPU)	Selectivity CO_2/N_2	Reference
Flat sheet [a]	Polysulfone	Functionalized carbon nano-fiber (CNF)	4.50	1.1	-----	32
Flat sheet [b]	Polysulfone	--------	22.01 ± 3.42	1.33 ± 0.59	16.5	33
Flat sheet [c]	Polysulfone	C15A 2.0 %	75.4 ± 6.20	17.74 ± 1.55	4.25	13
Flat sheet [c]	Polysulfone	GO (0.25 wt %)	76.04	6.21	12.24	This study

[a] P =2 bar at ambient temperature
[b] P = 4.48 bar feed pressure at ambient temperature
[c] P = 5 bar feed pressure and T= 25 °C

4. Conclusions

In the present study, three polysulfone solutions were prepared by the addition of graphene oxide (0.0, 0.25 and 0.05 % (w/w)). The membranes were fabricated through a phase separation process. Results indicated that adding graphene oxide to the polymer increased the viscosity and the surface roughness of the membrane. The addition of 0.25 % of graphene oxide to the polymer solution, caused the thickness of the selector layer to reduce from 132 nm to 86 nm. However, the increase of graphene oxide up to 0.50 % increased the selector layer thickness to 102 nm. The pure polysulfone membrane showed a more porous surface morphology compared to MMMs. By the addition of graphene oxide, the glass transition temperature increased significantly, indicating strong bonds between the polysulfone and graphene oxide. It is concluded that the addition of graphene oxide improved the thermal stability. As per the gas separation experiments, the permeation flux of carbon dioxide was 61.22 GPU for the pure membrane, whereas it reached 76.04 GPU by adding 0.25 % of graphene oxide to the polymer matrix. The N_2 permeation flux was lower than that of carbon dioxide, where it was 10.93 GPU for the pure membrane and 3.91 GPU for the membrane fabricated with 0.5 % of graphene oxide. The methane gas permeation flux was 11.31 GPU for the pure membrane and reached to 6.95 GPU and 4.92

GPU for the membranes fabricated with 0.25 % and 0.5 % of graphene oxide respectively. For M1, M2 and M3 membranes, the carbon dioxide selectivities versus nitrogen were 5.60, 12.24 and 17.79 respectively. Carbon dioxide gas selectivities versus methane for M1, M2 and M3 membranes were 5.41, 10.94 and 14.14 respectively.

References

[1] Kuila, T., Bose, S., Mishra, A. K., Khanra, P., Kim, N. H. and Lee, J. H., "Chemical functionalization of graphene and its applications", *Progress in Materials Science*, **57**, 1061 (2012).

[2] Yang, X., Wang, X., Yang, J., Li, J. and Wan, L., "Functionalization of graphene using trimethoxysilanes and its reinforcement on polypropylene nanocomposites", *Chemical Physics Letters*, **570**, 125 (2013).

[3] Li, X., Cheng, Y., Zhang, H., Wang, S., Jiang, Z., Guo, R. and Wu, H., "Efficient CO_2 capture by functionalized graphene oxide nanosheets as fillers to fabricate multi-permselective mixed matrix membranes", *ACS Applied Materials & Interfaces*, **7** (9), 5528 (2015).

[4] Checchetto, R., Miotello, A., Nicolais, L. and Carotenuto, G., "Gas transport through nanocomposite membrane composed by polyethylene with dispersed graphite nanoplatelets", *Journal of Membrane Science*, **463**, 196 (2014).

[5] Liu, H., Huang, W., Yang, X., Dai, K., Zheng, G., Liu, C., Shen, C., Yan, X., Guo, J. and Guo, Z., "Organic vapor sensing behaviors of conductive thermoplastic polyurethane–graphene nanocomposites", *Journal of Materials Chemistry, C*, **4**, 4459 (2016).

[6] Ganesh, B. M., Isloor, A. M. and Ismail, A. F., "Enhanced hydrophilicity and salt rejection study of graphene oxide-polysulfone mixed matrix membrane", *Desalination*, **313**, 199 (2013).

[7] Yadav, M., Rhee, K. Y. and Park, S. J., "Synthesis and characterization of graphene oxide / carboxymethylcellulose / alginate composite blend films", *Carbohydrate Polymers*, **110**, 18 (2014).

[8] Wang, Y., He, Q., Qu, H., Zhang, X., Guo, J., Zhu, J., Zhao, G., Colorado, H. A., Yu, J., Sun, L., Bhana, S., Khan, M. A., Huang, X., Young, D. P., Wang, H., Wang, X., Wei, S. and Guo, Z., "Magnetic graphene oxide nanocomposites: nanoparticles growth mechanism and property analysis", *Journal of Materials Chemistry, C*, **2**, 9478 (2014).

[9] Liu, H., Li, Y., Dai, K., Zheng, G., Liu, C., Shen, C., Yan, X., Guo, J. and Guo, Z., "Electrically conductive thermoplastic elastomer nanocomposites at ultralow graphene loading levels for strain sensor applications" *Journal of Materials Chemistry, C*, **4**, 157 (2016).

[10] Zhao, L., Cheng, C., Chen, Y. F., Wang, T., Du, C. H. and Wu, L. G., "Enhancement on the permeation performance of polyimide mixed matrix membranes by incorporation of graphene oxide with different oxidation degrees", *Polymers for Advanced Technologies*, **26** (4), 330 (2015).

[11] Ionita, M., Pandele, A. M., Crica, L. and Pilan, L., "Improving the thermal and mechanical properties of polysulfone by incorporation of graphene oxide", *Composites Part B: Engineering*, **59**, 133 (2014).

[12] Zulhairun, A. K., Ng, B. C., Ismail, A. F., Surya Murali, R. and Abdullah, M. S., "Production of mixed matrix hollow fiber

membrane for CO_2/CH_4 separation", *Separation and Purification Technology*, **137**, 1 (2014).

[13] Zulhairun, A. K., Ismail, A. F., Matsuura, T., Abdullah, M. S. and Mustafa, A., "Asymmetric mixed matrix membrane incorporating organically modified clay particle for gas separation", *Chemical Engineering Journal*, **241**, 495 (2014).

[14] Zulhairun, A. K. and Ismail, A. F., "The role of layered silicate loadings and their dispersion states on the gas separation performance of mixed matrix membrane", *Journal of Membrane Science*, **468**, 20 (2014).

[15] Kim, S., Chen, L., Johnson, J. K. and Marand, E., "Polysulfone and functionalized carbon nanotube mixed matrix membranes for gas separation: Theory and experiment", *Journal of Membrane Science*, **294** (1-2), 147 (2007).

[16] Zhao, Y., Ding, H. and Zhong, Q., "Preparation and characterization of aminated graphite oxide for CO_2 capture", *Applied Surface Science*, **258** (10), 4301 (2012).

[17] Md Nordin, N. A. H., Racha, S. M., Matsuura, T., Misdan, N., Abdullah Sani, N. A., Ismail, A. F. and Mustafa, A., "Facile modification of ZIF-8 mixed matrix membrane for CO_2/CH_4 separation: Synthesis and preparation", *RSC Advances*, **5** (54), 43110 (2015).

[18] Md Nordin, N. A. H., Ismail, A. F., Mustafa, A., Surya Murali, R. and Matsuura, T., "The impact of ZIF-8 particle size and heat treatment on CO_2/CH_4 separation using asymmetric mixed matrix membrane", *RSC Advances*, **4** (94), 52530 (2014).

[19] Shen, J., Zhang, M., Liu, G., Guan, K. and Jin, W., "Size effects of graphene oxide on mixed matrix membranes for CO_2 separation", *AIChE Journal*, **62** (8), 2843 (2016).

[20] Zahri, K., Wong, K. C., Goh, P. S. and Ismail, A. F., "Graphene oxide/ polysulfone hollow fiber mixed matrix membrane for gas separation", *RSC Advances*, **6** (92), 89130 (2016).

[21] Mahmoud, K. A., Mansoor, B., Mansour, A. and Khraisheh, M., "Functional graphene nanosheets: The next generation membranes for water desalination", *Desalination*, **356**, 208 (2015).

[22] Chang, D. W., Choi, H. -J., Jeon, I. -Y., Seo, J. M., Dai, L. and Baek, J. B., "Solvent-free mechanochemical reduction of graphene oxide", *Carbon*, **77**, 501 (2014).

[23] Wu, T., Wang, X., Qiu, H., Gao, J., Wang, W. and Liu, Y., "Graphene oxide reduced and modified by soft nanoparticles and its catalysis of the Knoevenagel condensation", *Journal of Materials Chemistry*, **22** (11), 4772 (2012).

[24] Thi Vu, T. H., Thi Tran, T. T., Thi Le, H. N., Thi Nguyen, P. H., Bui, N. Q. and Essayem, N., "A new green approach for the reduction of graphene oxide nanosheets using caffeine", *Bulletin of Materials Science*, **38** (3), 667 (2015).

[25] Loryuenyong, V., Totepvimarn, K., Eimburanapravat, P., Boonchompoo, W. and Buasri, A., "Preparation and characterization of reduced graphene oxide sheets via water-based exfoliation and reduction methods", *Advances in Materials Science and Engineering*, **2013**, Article ID 923403, (2013).

[26] Rahbari-Sisakht, M., Ismail, A. F., Rana, D. and Matsuura, T., "A novel surface modified polyvinylidene fluoride hollow

fiber membrane contactor for CO_2 absorption", *Journal of Membrane Science*, **415-416**, 221 (2012).

[27] Lan, Y., Liu, H., Cao, X., Zhao, S., Dai, K., Yan, X., Zheng, G., Liu, C., Shen, C. and Guo, Z., "Electrically conductive thermoplastic polyurethane/ polypropylene nanocomposites with selectively distributed graphene", *Polymer*, **97**, 11 (2016).

[28] Aditya Kiran, S., Lukka Thuyavan, Y., Arthanareeswaran, G., Matsuura, T. and Ismail, A. F., "Impact of graphene oxide embedded polyethersulfone membranes for the effective treatment of distillery effluent", *Chemical Engineering Journal*, **286**, 528 (2016).

[29] Nwanonenyi, S. C., Obidiegwu, M. U. and Onuegbu, G. C., "Effects of particle sizes, filler contents and compatibilization on the properties of linear low density polyethylene filled periwinkle shell powder", *The International Journal of Engineering and Science (IJES)*, **2** (2), 1 (2013).

[30] Hashemifard, S. A., Ismail, A. F. and Matsuura, T., "Mixed matrix membrane incorporated with large pore size halloysite nanotubes (HNTs) as filler for gas separation: Morphological diagram", *Chemical Engineering Journal*, **172** (1), 581 (2011).

[31] Baker, R. W., Membrane technology and applications, 3rd edition, Wiley, p. 11 (2012).

[32] Kiadehi, A. D., Jahanshahi, M., Rahimpour, A. and Ghoreyshi, S. A. A., "The effect of functionalized carbon nano-fiber (CNF) on gas separation performance of polysulfone (PSf) membranes", *Chemical Engineering and Processing: Process Intensification*, **90**, 41 (2015).

[33] Junaidi, M. U. M., Leo, C. P., Kamal, S. N. M., Ahmad, A. L. and Chew, T. L., "Carbon dioxide removal from methane by using polysulfone/SAPO-44 mixed matrix membranes", *Fuel Processing Technology*, **112**, 1 (2013).